Journal of Nondestructive Evaluation

Vol. 3, No. 3 September 1982

1983

CONTENTS

Journal of Nondestructive Evaluation, Vol. 3, No. 3, 1983

Finite Element Modeling of Absolute Eddy Current Probe Signals

N. Ida,[1] K. Betzold,[2] and W. Lord[1]

Received January 21, 1983

Finite element analysis techniques are applied to the problem of predicting signals from an absolute eddy current probe in the tube sheet region of a PWR steam generator for the purpose of optimizing the probe coil geometry and determining the feasibility of using such a probe to characterize the condition of the tube and tube sheet crevice.

KEY WORDS: finite element modeling; eddy current; absolute probe; steam generator tubing; NDE.

1. INTRODUCTION

Numerical analysis techniques, primarily finite difference and finite element methods, have been used for some time to study dc and low frequency electromagnetic fields in electrical machinery.[1-4] A number of advantages have been shown to favor the finite element approach for such studies,[5] including ease of handling boundary conditions, ability to follow awkward boundary shapes, and relative economy of computer facilities usage. These factors are particularly relevant for the simulation of electromagnetic nondestructive testing techniques, and hence parallel developments have taken place in the use of finite element analysis for modeling eddy current and active and residual leakage field NDT phenomena.[6-10]

Such models are important in understanding (visualizing) the physics of electromagnetic field/defect interactions, designing NDT test rigs and probes, developing training data for automated defect characterization schemes, and simulating those testing situations (such as in a PWR steam generator) which are difficult and/or expensive to replicate in the laboratory. This paper illustrates the application of an axisymmetric finite element code to the problem of designing an absolute eddy current probe for use in the tube sheet region of PWR steam generators. The code is used to study different probe sizes and to determine the probe responses to various sludge deposits in the crevice gap.

2. GOVERNING ELECTROMAGNETIC FIELD EQUATIONS

The relevant Maxwell equations governing the eddy current phenomena in conducting materials are

$$\nabla \times \bar{H} = \bar{J} \tag{1}$$

$$\nabla \times \bar{E} = -\frac{\partial \bar{B}}{\partial t} \tag{2}$$

$$\Delta \cdot \bar{B} = 0 \tag{3}$$

where in Eq. (1) the conduction current density $\bar{J}$ is assumed to be dominant (i.e., low frequency assumption), and therefore the displacement current is neglected. Together with the relation $\bar{B} = \mu \bar{H}$, Eq. (1) can be rewritten

$$\nabla \times \bar{H} = \sigma \bar{E} \tag{4}$$

[1]Electrical Engineering Department, Colorado State University, Fort Collins, CO 80523.
[2]Fraunhofer Institut für Zerstörungsfreie Prüfverfahren.

The magnetic flux density $\bar{B}$ can be defined in terms of the magnetic vector potential

$$\bar{B} = \nabla \times \bar{A} \tag{5}$$

and Eq. (2) can be rewritten as

$$\nabla \times \bar{E} = -\nabla \times \frac{\partial \bar{A}}{\partial t} \tag{6}$$

or

$$\bar{E} = -\frac{\partial \bar{A}}{\partial t} - \nabla\phi \tag{7}$$

where ϕ is the electric scalar potential due to any existing current source $\bar{J}_s$,

$$\bar{J}_s = -\sigma\nabla\phi \tag{8}$$

Using the relation $\bar{J} = \sigma\bar{E}$ and expressing Eq. (1) in terms of $\bar{A}$,

$$\frac{1}{\mu}(\nabla \times \nabla \times \bar{A}) = \bar{J}_s - \sigma\frac{\partial \bar{A}}{\partial t} \tag{9}$$

Assuming a sinusoidal steady state source and using the relation $\nabla \times \nabla \times \bar{A} = -\nabla^2\bar{A} + \nabla(\nabla \cdot \bar{A})$, Eq. (9) becomes

$$\left(\frac{1}{\mu}\right)\nabla^2\bar{A} = -\bar{J}_s + j\omega\sigma\bar{A} \tag{10}$$

where ω is the angular frequency of the source. Here the divergence of the magnetic potential is taken as zero, $(\nabla \cdot \bar{A}) = 0$, a known property of two-dimensional fields. This is the linear diffusion equation for the sinusoidal steady-state condition.

In axisymmetric geometries, this equation can be written in a cylindrical coordinate system (r, θ, z)[1]:

$$\frac{1}{\mu}\left(\frac{\partial^2\bar{A}}{\partial r^2} + \frac{1}{r}\frac{\partial \bar{A}}{\partial r} + \frac{\partial^2\bar{A}}{\partial z^2} - \frac{A^2}{r^2}\right) = -\bar{J}_s + j\omega\sigma\bar{A} \tag{11}$$

where $\bar{J}_s$ and the vector potential $\bar{A}$ have components only in the positive θ direction. At the same time the induced current density $\bar{J}_e$ has components in the negative θ direction:

$$\bar{J}_e = -j\omega\sigma\bar{A} \tag{12}$$

For a given geometry the magnetic vector potential can be found by solving Eq. (11) with appropriate boundary conditions.

3. THE FINITE ELEMENT FORMULATION

Instead of solving Eq. (11) directly, variational principles can be utilized to show that the correct solution of Eq. (11) is obtained by minimizing the energy related functional,[2,3]

$$F(A) = \int_v \left[\frac{1}{\mu}BdB + \frac{1}{2}j\omega\sigma|A|^2 - J_s \cdot A\right] dv \tag{13}$$

The solution now consists of finding a set of functions A such that the energy related functional is minimized. Because this cannot be done everywhere in space, a bounded region (solution region) is discretized into a large number of linear triangular elements. In each element three nodal points are defined at which the magnetic vector potential is found. The value of A within each element is assumed to be a linear combination of the nodal values A_i[4,5]:

$$A(r, z) = \frac{1}{2\Delta}\sum_{i=1}^{3}(a_i + b_i r + c_i z)A_i \tag{14}$$

where Δ is the area of the element, and A_i are the nodal values of the magnetic vector potential. This approximation is extended throughout the solution region resulting in N nodal points and therefore in N unknown values of A.

Minimization of the energy functional is achieved by setting the partial derivative with respect to each nodal value equal to zero:

$$\frac{\partial F(A)}{\partial A_k} = 0 \qquad k = 1, 2, \ldots, N \tag{15}$$

For convenience, this operation is performed element by element. The approximation for the magnetic vector potential in Eq. (14) is substituted into the energy functional and the derivatives with respect to the three nodes set to zero. This results in three equations which in matrix form can be written as

$$[[S]_e + j[R]_e]\{A\}_e = \{Q\}_e \tag{16}$$

$[S]$ is the 3×3 real part of the elemental matrix

consisting of geometrical quantities of the mesh (r and z values of the element vertices, the area of the element and permeability) and represents the left-hand side of Eq. (11). $[R]$ is the 3×3 imaginary part of the matrix and consists of the values of conductivity (σ), angular frequency (ω), and area of the element, and represents the second term in the right-hand side of Eq. (11). $\{Q\}$ is the 3×1 vector of contributions at the nodes of the element from the impressed current densities (J_s), and $\{A\}$ is the 3×1 vector of unknown values of the magnetic vector potential at the nodes of the element.

This elemental system of equations is the basic finite element representation of the energy functional. Each such elemental matrix is summed into a global system of equations

$$[G]\{A\} = \{Q\} \tag{17}$$

where $[G]$ is the $N \times N$ banded symmetric complex global matrix, and $\{Q\}$ and $\{A\}$ are the $N \times 1$ complex source matrix and the $N \times 1$ complex vector of unknowns, respectively. The Gauss elimination algorithm is applied to this system of equations, taking advantage of the symmetry and bandwidth, to solve for A at the nodes of the finite element mesh. From the magnetic vector potential other quantities can be calculated, such as flux densities using Eq. (5).

4. IMPEDANCE OF EDDY CURRENT COILS

In NDT applications, the signals from eddy current probes carry information concerning the probe's environment, changes in which cause variations in the probe impedance. The coil impedance can be calculated directly from the complex magnetic vector potential.[10] The impedance of a circular loop of radius r_i carrying a current I_s is

$$\bar{z}_i = \frac{j\omega 2\pi r_i \bar{A}_i}{\bar{I}_s} \tag{18}$$

where $\bar{A}_i$ is the value of the magnetic vector potential at r_i.

Integration of this equation over the cross-section of the coil yields the impedance of the coil. Since the values of A are not known at the location of each turn in the coil, an average value is taken as representing the magnetic vector potential in each element. This value is associated with the centroid of the element, the radius of the loop being r_c. Then assuming N_s to be a uniform turn density, the impedance of the coil is

$$\bar{z} = \frac{j\omega 2\pi N_s}{\bar{I}_s} \sum_{j=1}^{N_c} r_{cj} A_{cj} \Delta_j \tag{19}$$

or, since $N_s \bar{I}_s = \bar{J}_s$,

$$\bar{z} = \frac{j\omega 2\pi \bar{J}_s}{I_s^2} \sum_{j=1}^{N_c} (r_{cj}\Delta_j)\bar{A}_{cj} \tag{20}$$

where N_c is the number of elements in the cross-section of the coil. In many applications it is customary to normalize the impedance by dividing it with the reactance of the coil in free space, resulting in the normalized impedance

$$z_n = \frac{z}{\omega L_0} \tag{21}$$

5. RESULTS

The method presented in this paper has been applied to the study of three problems related to the nondestructive testing of steam generator geometries with eddy current probes:

1. Optimization of coil geometries for maximum sensitivity
2. Detection of foreign materials in a known environment
3. Detection of geometrical irregularities

Figure 1 is a diagram of the geometry studied. It is a section of a steam generator's Incoloy 800 tube inside the tube sheet region. The steam generator (German design) has rolled tubes where the rolling region can be at varying distances from the tube sheet inner surface (l in Fig. 1). The crevice gap between the tube and tube sheet accumulates foreign materials (mostly copper and magnetite), the detection and classification of which is desirable. The absolute coil, 1 mm thick, has a length of l mm, which needs to be optimized for the particular application. In addition the signal from the rolling region is to be modeled for identification of the tube condition.

The geometry in Fig. 1 was discretized into 10,440 triangular elements with a total of 5430 nodes,

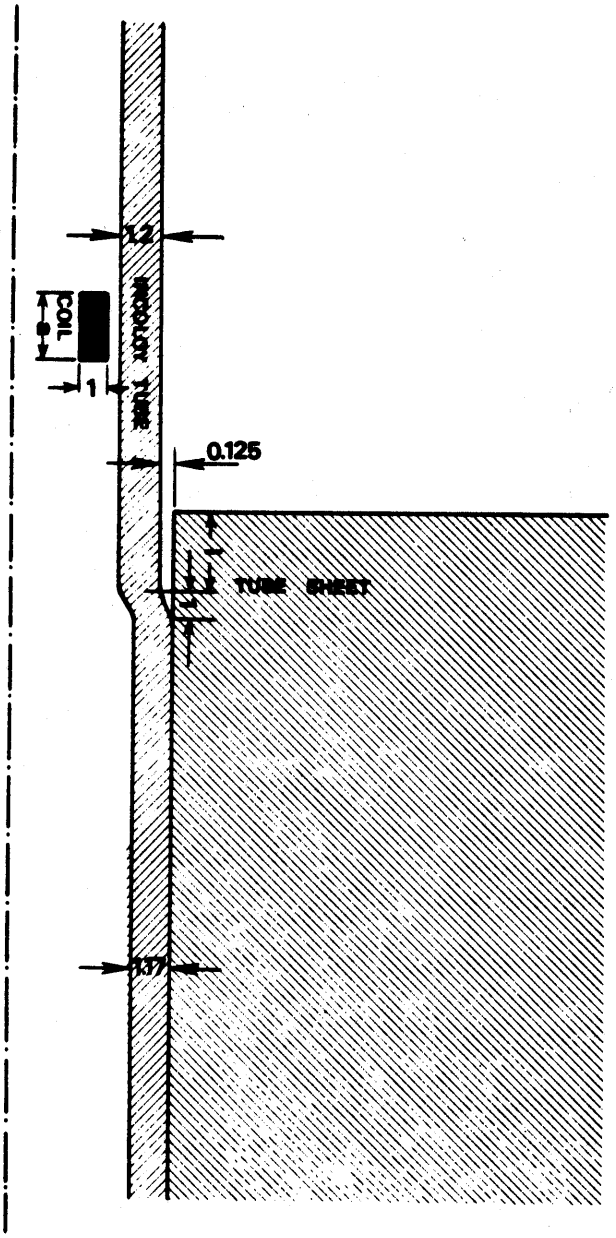

Fig. 1. Geometry of steam generator section showing the tube sheet, tube, and coil. Dimensions are in millimeters.

the central portion of which is shown in Fig. 2. To determine the probe length needed to obtain the best signal for different locations of the rolling region relative to the tube sheet surface, three coil lengths ($a = 1$, 3, and 9 mm) were modeled each for three distances l ($l = 1$, 3, and 9 mm). For each situation (9 in all) the corresponding probe is positioned at some distance from the tube sheet such that the effect of the tube sheet or rolling region is negligible. A finite element solution is obtained for this position and the impedance calculated. The probe is next moved to a new position (one layer of elements lower) and the process repeated. The probe is moved in this way in 91 steps for each of the 9 situations above to produce the curves in Fig. 3.

It is clear from this figure that the longer the coil in comparison with the distance between the two factors that cause the change in the signal (tube sheet and rolling region), the less distinct are the two phenomena in the signal. Thus in a coil 9 mm long, testing for the rolling region, which is only 1 mm away from the tube sheet surface, produces a flat composite signal in which the rolling and the tube sheet cannot be distinguished, as in Fig. 3(g). The other extreme is when the coil is much smaller than the distance l, as in Fig. 3(c). Here the two signals are simply superimposed as one signal doesn't affect the other.

The curves in Fig. 3 are generated at 100 kHz and are, in general, a composite signal. The lower, comma-shaped part of the curve is due to the effect of the tube sheet, and the upper, "s" shaped part is due to the rolling region. These curves compare very well with experimental results such as the curve in Fig. 4, taken at 100 kHz. The choice of coil shape might be complicated by additional factors such as the minimum number of required turns, but as can be seen from these results, the coil should be of the same general length as the effect it is measuring. Since the average distance of the rolling region is about 3 mm, a coil length of 3 mm would be a good choice. For this reason, the rest of the situations modeled in this work use this size coil. Figure 5 shows this coil and the field distribution around it in the vicinity of the tube sheet and rolling region. A second significant problem relating to nondestructive testing is the identification of foreign materials, and more importantly, the distinction between changes in the coil output due to these materials and other parameters such as defects or geometrical anomalies. In applications such as testing of steam generators, one common situation is the accumulation of copper and magnetite deposits in the crevice gap between the tube and tube sheet. Because of the narrowness of the gap and the unknown exact composition of the materials, the numerical model is of significance in studying these parameters.

The crevice gap was first studied with magnetite and then with copper flush with the tube sheet. The signals from these simulations are shown in Figs. 6(b) and 6(e), respectively. A distinct change in the signal

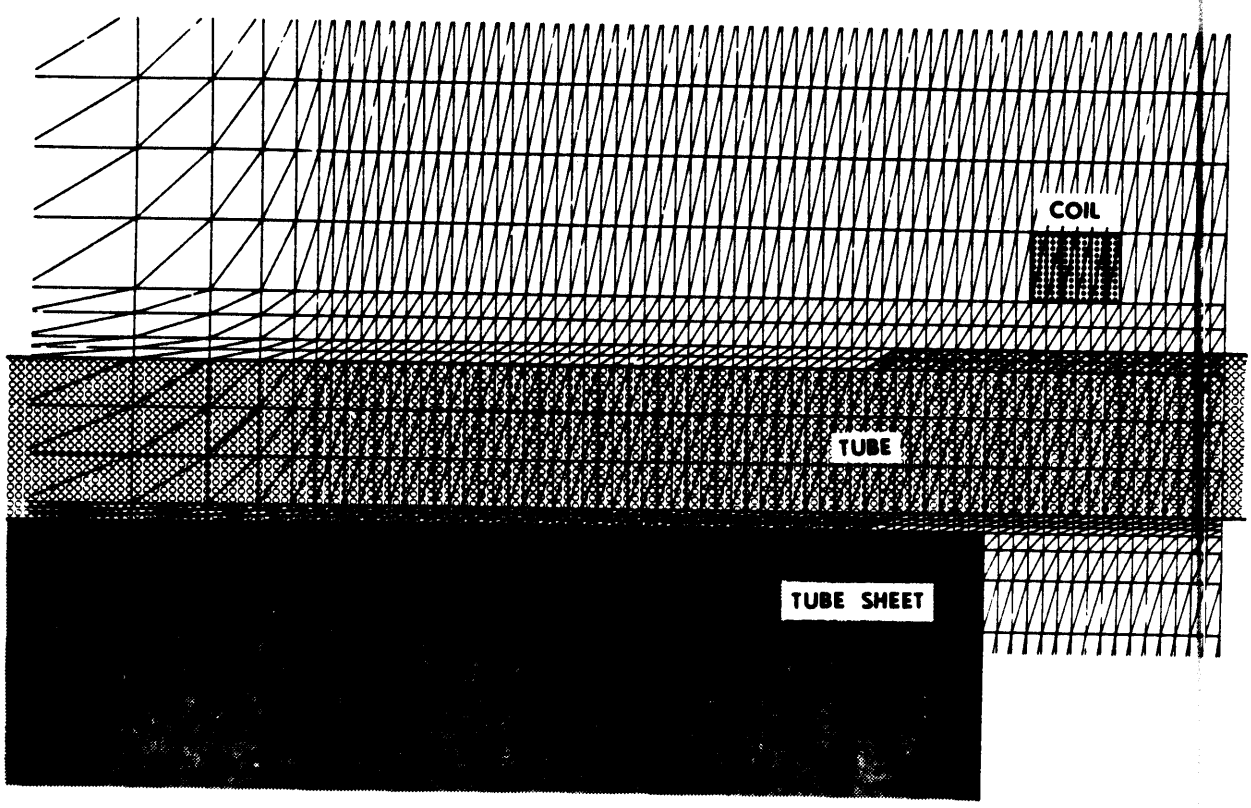

Fig. 2. Portion of the mesh showing the central part of the region discretized.

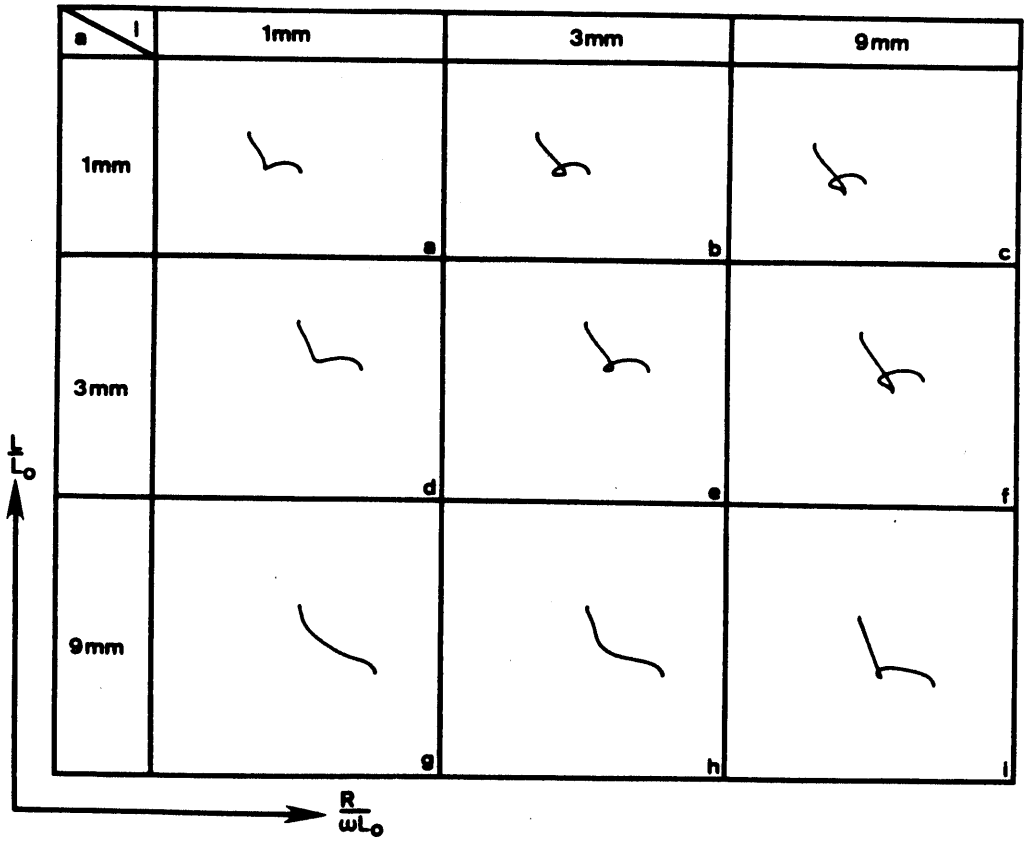

Fig. 3. Impedance plane trajectories of different coils (1, 3, and 9 mm long) and different spacings between tube sheet and rolling (1, 3, and 9 mm).

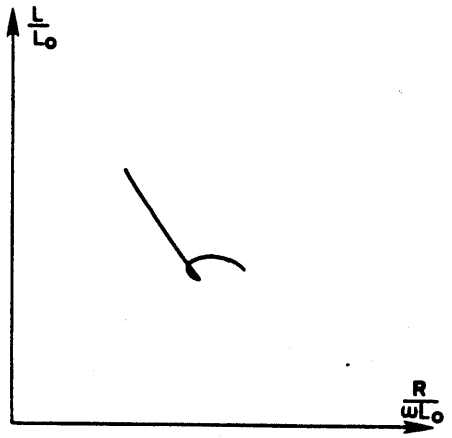

Fig. 4. Experimental impedance plane trajectory from a 3 mm long coil at nominal spacing of the tube sheet and rolling at 100 kHz.

compared to the clean crevice gap in Fig. 6(a) is apparent, especially in the case of copper. The second simulation studied is with the crevice gap filled and a ring of 2 mm thickness above the gap to represent the common ridge or pile up of foreign material found in steam generators. Figure 6(c) is the signal from magnetite and Fig. 6(f) from copper pile up. Figures 6(d) and 6(g) are similar to 6(c) and 6(f), but only the ring of foreign material is present while the crevice gap is clean. From the signals in Fig. 6 it is clear that foreign materials can be detected and classified by their signals.

The relation of the different signals obtained for the crevice gap condition is summarized in Fig. 7 for a nominal condition of the tube sheet and rolling region (the rolling region is 3 mm from the tube sheet surface). Each signal is distinct and unique. Figures 3 and 6 also show that these signals tend to mask the original information, in this case the crevice gap and the tube sheet to the extent that their presence might not be identifiable. Especially troublesome is the presence of copper due to its higher conductivity. Simulations of mixtures of copper and magnetite can also be performed by varying the conductivity and permeability of the mixture.

6. CONCLUSIONS

Finite element analysis techniques, originally developed for studying electromagnetic fields in electrical machinery, can be used to examine eddy cur-

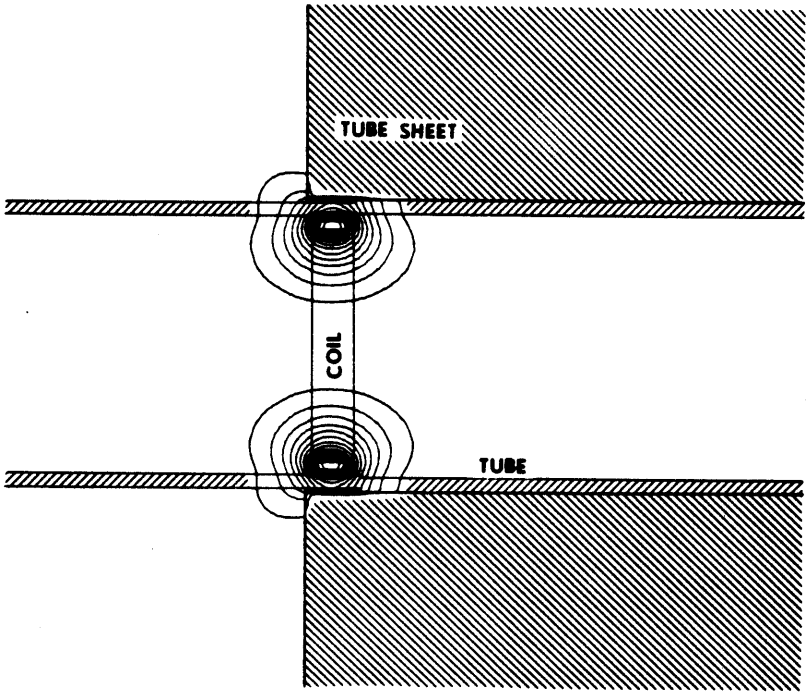

Fig. 5. Magnetic field contours of a 3 mm coil in the vicinity of the crevice gap and rolling region.

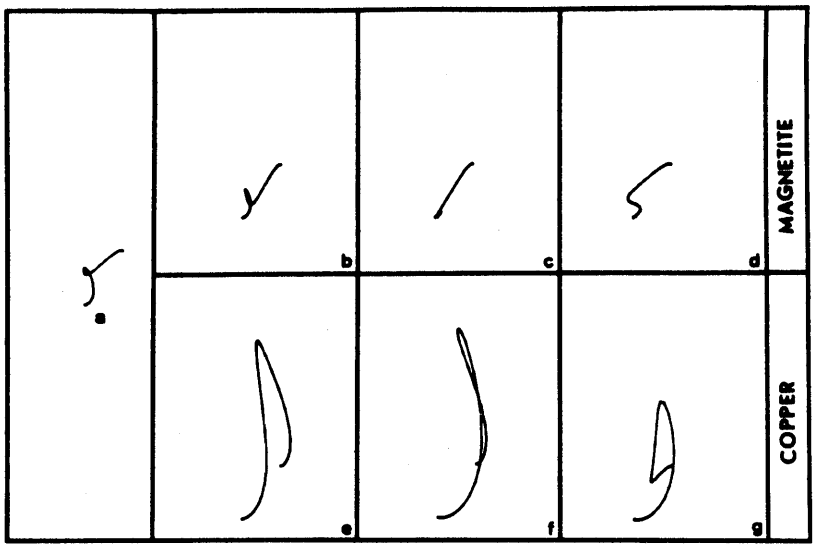

Fig. 6. Signals from copper and magnetite in the crevice gap.

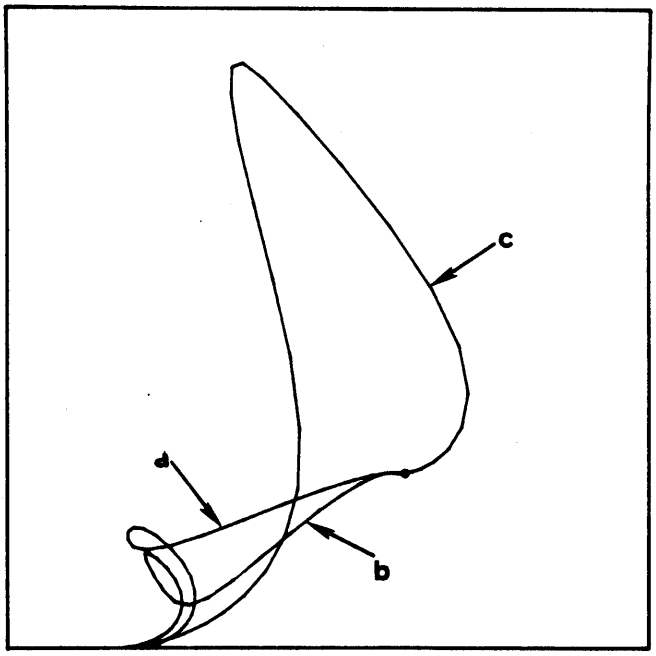

Fig. 7. Relation between signals from different conditions in the crevice gap: (a) clean crevice gap; (b) crevice gap filled with magnetite; (c) crevice gap filled with copper.

rent NDT phenomena. This paper describes the finite element technique and shows how it can be applied to the problem of predicting absolute eddy current probe signals in a PWR steam generator. From a computational point of view, the steam generator geometry is somewhat unique in that it is symmetrical about a tube axis, thus simplifying the computations. For more complex geometries, a full three-dimensional treatment will be necessary in order to predict eddy current probe signals. Nevertheless, one can conclude from this work that numerical analysis methods will play an increasing role in the

simulation of eddy current NDT phenomena, particularly with regard to designing probes and modeling those testing situations difficult to replicate in a laboratory.

ACKNOWLEDGMENTS

This work was supported by the Electric Power Research Institute and the Bundesministerium für Forschung und Technologie.

REFERENCES

1. J. Donea, S. Giulinai, and A. Philippe, Finite elements in the solution of electromagnetic induction problems, *Int. J. Numer. Methods Eng.* **8**: 359–367 (1974).
2. E. A. Erdelyi et al., Nonlinear magnetic field analysis of DC machines, *IEEE Trans. Power Apparatus Syst.* **89**: 1546–1583 (1970).
3. P. Silvester and M. V. K. Chari, Finite element solution of saturable magnetic field problems, *IEEE Trans. Power Apparatus Syst.* **89**: 1642–1651 (1970).
4. O. W. Anderson, Transformer leakage flux program based on the finite element method, *IEEE Trans. Power Apparatus Syst.* **92**: 682–689 (1973).
5. N. A. Demerdash and T. W. Nehl, An evaluation of the methods of finite elements and finite differences in the solution of nonlinear electromagnetic fields in electrical machines, *IEEE Trans. Power Apparatus Syst.*, Vol. **98**(1): 74–87 (1979).
6. W. Lord and J. H. Hwang, Finite element modeling of magnetic field defect interactions, *ASTM J. Test. Eval.* **3**(1): 21–25 (1975).
7. W. Lord and J. H. Hwang, Defect characterization from magnetic leakage fields, *Br. J. Nondestr. Test.* **19**(1): 14–18 (1977).
8. W. Lord, J. M. Bridges, W. Yen, and R. Palanisamy, Residual and active leakage fields around defects in ferromagnetic materials, *Mat. Eval.* **36**(8): 47–54 (1978).
9. W. Lord, A survey of electromagnetic methods of nondestructive testing, in *Mechanics of Nondestructive Testing*, W. W. Stinchcomb, ed. (Plenum Press, New York, 1980), pp. 77–100.
10. R. Palanisamy and W. Lord, Finite element modeling of electromagnetic NDT phenomena, *IEEE Trans. Magnetics* **MAG-15**(6): 1479–1481 (1979).

Volume 3, Number 3

September 1982

JNOED5 3(3) 125–182 (1982)

ISSN 0195-9298

Journal of Nondestructive Evaluation

Plenum Press · New York and London